Available online at www.sciencedirect.com
ScienceDirect
Mathematics and Computers in Simulation 81 (2010) 899–914
MATHEMATICS AND COMPUTERS IN SIMULATION
www.elsevier.com/locate/matcom

Original article

Border collision bifurcations in one-dimensional linear-hyperbolic maps

Laura Gardini [a], Fabio Tramontana [a,*], Iryna Sushko [b]

[a] Università degli Studi di Urbino, Department of Economics and Quantitative Methods, Via Saffi 42, 61029 Urbino, Italy
[b] Institute of Mathematics, National Academy of Sciences of Ukraine, and Kiev School of Economics, Kiev, Ukraine

Received 10 August 2009; received in revised form 28 August 2010; accepted 11 October 2010
Available online 13 November 2010

Abstract

In this paper we consider a continuous one-dimensional map, which is linear on one side of a generic kink point and hyperbolic on the other side. This kind of map is widely used in the applied context. Due to the simple expression of the two functions involved, in particular cases it is possible to determine analytically the border collision bifurcation curves that characterize the dynamic behaviors of the model. In the more general model we show that the steps to be performed are the same, although the analytical expressions are not given in explicit form.

Keywords: Piecewise smooth map; Border-collision bifurcation; Bistability

1. Introduction

In recent years a significant amount of papers have been published regarding piecewise smooth (PWS) systems because of their wide use in applications. Several models in engineering and physical sciences are described by PWS systems (see [1,3,6–8,12–14,16,17,24,25,30,38]), as well as in economics (see [28,29]). The first results on PWS systems date back to several years ago, not only for continuous models but also for discontinuous systems [2,18,19,23], and are extended also to two-dimensional models (see [5,31,34,39,40]).

The main point in the analysis of PWS systems is the occurrence of *border collision bifurcations* (BCB), due to the merging (or collapse) of some invariant set (a fixed point, a periodic point of a cycle, or the boundary of any invariant set) with the kink point in which the function changes its definition. This may lead to a drastic change, unexpected (i.e. impossible) in the framework of smooth systems. Such border collision bifurcations are responsible, for example, for the direct transition from regular regime to chaotic dynamics, or to divergence [6,20–22,26,27].

The analysis of the effect of a collision of an invariant set with a kink point, a boundary for the map definition, in general is not an easy task. It is a bifurcation which depends on the shape of the map on the two sides of the collision, and may lead to several different dynamic effects. For example, the dynamics can change suddenly from an attracting fixed point to an attracting cycle of any period, or to chaotic dynamics (true chaos or strict chaos following [11], for a full measure chaotic set, and robust chaos following [4], because the chaotic set is persistent as a function of the parameters).

* Corresponding author.
E-mail addresses: laura.gardini@uniurb.it (L. Gardini), f.tramontana@univpm.it (F. Tramontana), sushko@imath.kiev.ua (I. Sushko).

0378-4754/$36.00
doi:10.1016/j.matcom.2010.10.001

Limiting our interest to one-dimensional models, to our knowledge the only case in which all possible dynamics have been completely understood is the one-dimensional piecewise linear continuous map. The results are shown in a few papers [6,20–22,26,27].

Indeed, the results of the piecewise linear map are not as well known as the importance of that model requires. In fact, it represents a normal form which may also be used in the analysis of BCB occurring in smooth maps, leading to possible predictions of the dynamic effect of a collision. That is, given any piecewise smooth map with one kink point, the effect of a BCB is generally considered unpredictable, while it is really totally predictable using the piecewise linear map in canonical form. This is due to the fact that the dynamic result is simply associated with the derivatives of the smooth functions defined before and after the kink point, at the two sides of the kink point. This kind of analysis has been used for example in [15,32,33]. This clearly refers only to the result of the crossing of a fixed point, or of a k-cycle (which is considered as a fixed point for a suitable power of the map, the k-th iterate), through the kink point.

Here we shall extend the full analysis (in the parameter space) to a more general model. Still keeping one increasing branch linear on the left side of the kink point, we consider a smooth decreasing branch given by a hyperbola on the right side. We recall that PWS maps are used also to simulate C-bifurcations and grazing bifurcations in engineering models (see [12,14,24]). In fact, these maps occur when there is a border in the global Poincaré section for a flow (dynamic system in continuous time) such that points at the two sides of the border behave differently (are subject to different laws). This model, however, is used in some economic applications. It can be used to describe some simple financial relations between chartists and fundamentalists, as those recently called of “bull and bear dynamics” [36,37]. From the seminal papers by Day [9,10], such simple models are up to date for interpreting the financial crises. Another piecewise smooth model deduced from the same paper was represented by a linear branch on one side and a branch of quadratic (logistic function) on the other side. This model has been already studied in [32,33]. Here we adopt a different smooth function, from the analytic point of view (that is a hyperbola, as stated above), which is more coherent with the decreasing behavior required by the model described in [9,10]. In the general case the results are clear, but difficult to detect analytically in explicit form. A particular case, however, can be well studied. With this example as guideline, also the bifurcations of the general case can be understood and investigated.

There are several similarities to the results occurring in the one-dimen-sional piecewise linear continuous map. For example, due to the continuity of the map the fold (or tangent) bifurcations in PWS systems must always be associated with the appearance/disappearance of a pair of cycles.[1] The two cycles may be both unstable or one stable and one unstable. This also occurs in the case of a linear-logistic map, as considered in [32,33], and the fold bifurcations may be smooth saddle-node bifurcations (as the maximum may be in a smooth point). While in the linear-hyperbolic map under study, the role of the maximum in the kink point is the same as in the piecewise linear case: all the fold bifurcations are also border collision bifurcations.

We shall see that a BCB leading to the appearance/disappearance of a pair of k-cycles, for any $k \geq 3$, exists, and it may be associated with a saddle-node bifurcation (i.e. one stable cycle and one unstable), or with a saddle-saddle bifurcation (that is, both unstable cycles), thus leading directly to attractors given by cyclical chaotic intervals of period $2k$, k or 1. Remarkably, we shall see that all the k-cycles born stable via border collision will become unstable via a *degenerate flip bifurcation* (which means that at the bifurcation value all the points of some suitable interval are cycles of period $2k$ leaving only one k-cycle after the bifurcation) as occurs in piecewise linear maps (see also [35]). We recall that a standard flip bifurcation (supercritical or subcritical) is associated with a cycle of double period which is close to the bifurcating cycle (and changing the order of the crossing, the cycle of double period merges with the bifurcating one). While a degenerate flip bifurcation leads to a cycle of double period whose periodic points are located far from the bifurcating cycle. As we shall see, *how far* depends on the relative position of the kink point and the bifurcating cycle, because a degenerate flip bifurcation is also always a BCB. Moreover, while a standard flip bifurcation always gives rise (when supercritical) to a cycle of double period, a degenerate flip bifurcation may lead directly to cyclical chaotic intervals (of double period, or of the same period or a unique interval), as we shall see in the degenerate flip bifurcation of the fixed point in our model.

Besides the bifurcations of the cycles, we shall investigate the bifurcations involving the chaotic intervals. As expected, the bifurcations involving chaotic intervals are associated with the homoclinic bifurcations of the k-cycles born at the BCB (saddle-node or saddle-saddle). However, differently from the bifurcations occurring in the piecewise

[1] While a single cycle may appear in the case of a discontinuous map.

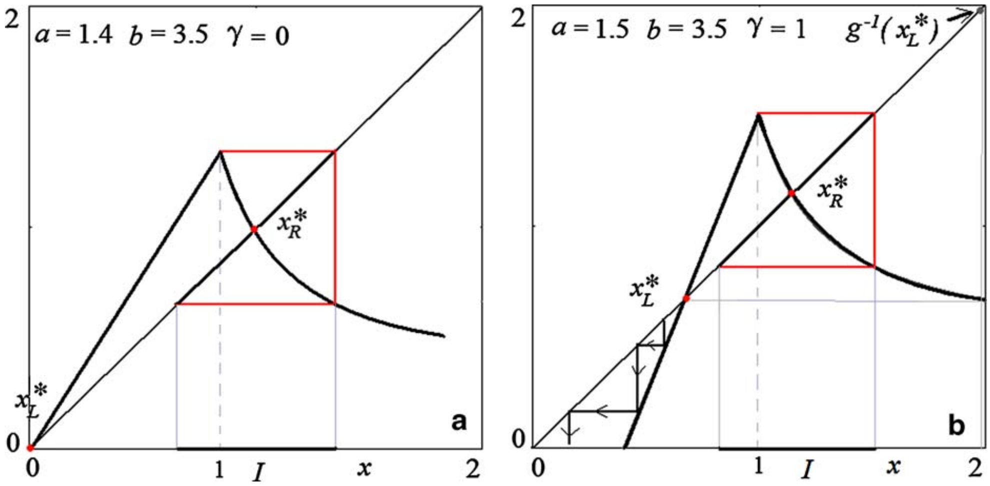

Fig. 1. Shape of the map (here in chaotic regime).

linear map, we shall see that the cyclical chaotic intervals of period 2^n cannot exist for any n. Instead, in the linear-hyperbolic map, the 2-cycle born by degenerate flip bifurcation will follow the same route to chaos as it occurs for the cycles of period $k \geq 3$, that is, the stable cycle is followed by cyclical chaotic intervals of period 4, 2 or 1.

We remark that also in the continuous one-dimensional Nordmark's map (even if it is represented by a linear branch and a smooth one with a square root nonlinearity, giving an infinite derivative in the kink point) the BCBs and the global (homoclinic) bifurcations can be detected using the same techniques used in this work (see e.g. [3]). In fact, a square root nonlinearity is not something peculiar in detecting the bifurcations associated with the appearance/disappearance of cycles. The BCB curves are determined by the images of the kink point as it occurs in other PWS systems, following the same steps used in the next sections. What differs with respect to the model under study is that in the Nordmark's map the flip bifurcations of the cycles are standard (not degenerate), subcritical or supercritical.

The study is structured as follows. In Section 2 we introduce the model, and the related properties associated with the bifurcations involving the fixed points and the 2-cycle. In Section 3 we deal with a simplified case, for which the BCB curves of the cycles and of the chaotic intervals are obtained analytically. The general case is considered in Section 4, where the implicit equations of the BCB curves are given. Section 5 concludes.

2. The model

The family of maps we are interested in is given by

$$y' = H(y) = \begin{cases} F(y) = ay + \gamma(y-p), & \text{if} \quad y \leq p \\ G(y) = \dfrac{ay}{1+B(y-p)}, & \text{if} \quad y \geq p \end{cases}$$

where $\gamma \geq 0, p \geq 1, 0 < a < B$. The function is continuous in the kink point (point of discontinuity in the first derivative), which can be fixed at 1 by rescaling the variable via the transformation $y = px$, so that we obtain, by setting $b = Bp$:

$$x' = T(x) = \begin{cases} f(x) = (a+\gamma)x - \gamma, & \text{if} \quad x \leq 1 \\ g(x) = \dfrac{ax}{1+b(x-1)}, & \text{if} \quad x > 1 \end{cases} \tag{1}$$

where

$$\gamma \geq 0, \quad 0 < a < b \tag{2}$$

Thus we have an increasing straight line for $x < 1$ and a decreasing branch of hyperbola for $x > 1$, with a positive horizontal asymptote ($0 < a/b < 1$). So all the dynamics are naturally confined in the positive range (i.e. we have always $x > 0$ when bounded absorbing intervals exist). The shape of the map (1) is shown in Fig. 1.

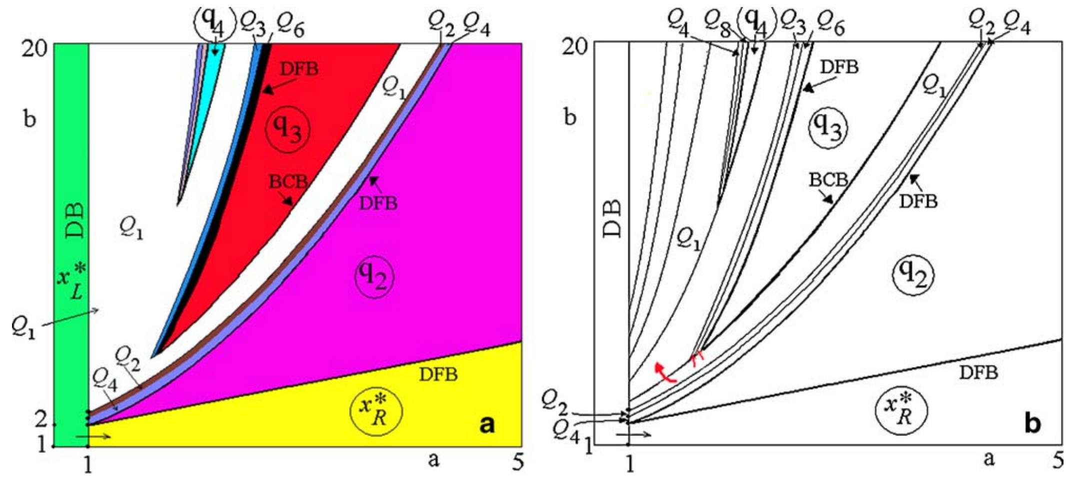

Fig. 2. Two-dimensional bifurcation diagram in the (a,b) parameter plane at $\gamma = 0$. In (a) there is only a numerical result. In (b) only analytical curves are drawn, whose equations are given in Section 3. In the periodicity regions for $k = 3, 4$ it can be seen that a BCB is saddle-node where the colors evidence the existence of a stable cycle, while it is saddle-saddle continuing the same curve.

From $f(0) = -\gamma < 0$ and $f(1) = g(1) = a$ we have that for $0 < a < 1$ the map has no fixed points, at $a = 1$ a *fold border collision bifurcation* occurs. It is called a fold bifurcation because as a crosses the value 1 this transition is from no fixed points to a pair of fixed points. It is a border collision because if we consider the bifurcation as the parameter a is decreased, for $\gamma > 0$, we can see that two fixed points (x_L^* and x_R^* in Fig. 1b) approach the kink point $x = 1$ and are merging in it at the bifurcation occurring for $a = 1$. What can we say about the dynamics occurring after this bifurcation? We may reach a regular regime, with a unique stable fixed point, globally attracting the bounded dynamics, or a chaotic regime. Thus this transition may be "smooth" or very much "dangerous" (leading to robust chaotic effects), and the dynamic behavior depends on the slopes of the two functions in the kink point at the bifurcation value. That is, using

$$\begin{aligned} f'(x) &= (a+\gamma) \\ g'(x) &= -\frac{a(b-1)}{[1+b(x-1)]^2} \end{aligned} \tag{3}$$

what occurs after, for $a > 1$, depends on the two values $f'(1) = (a + \gamma) > 0$ and $g'(1) = -a(b - 1) < 0$. As we can see, the result depends on three parameters. Being $\gamma \geq 0$, however, for any $a > 1$ the first derivative is $f'(1) > 1$ so that the fixed point x_L^* appearing on the left side of the kink point is certainly unstable. Differently, the other derivative $g'(1)$ depends on the values of two parameters, and the fixed point x_R^* appearing on the right side of the kink point may be locally stable or unstable. We shall see what kind of dynamics occur in the model when the second fixed point is also unstable and how such dynamics change as the parameters are varied in their range.

The uncertainty associated with border collision bifurcations is clear. For example, for $\gamma = 0$ the BCB occurring at $a = 1$ may lead to a globally stable fixed point when $1 < b < 2$ (so that $g'(1) \in (-1, 0)$), or to chaos when $b > 2$ (so that $g'(1) < -1$), and chaos may occur in k-cyclical chaotic intervals, with $k = 4$ or 2 or 1 as shown in Fig. 2. This also occurs for γ positive and close to 0.

In the next section we shall rigorously prove, in the case $\gamma = 0$, the BCBs associated with k-cycles and the bifurcations of chaotic intervals, which lead to the bifurcation scenarios summarized in the two-dimensional bifurcation diagram in the (a, b) parameter plane shown in Fig. 2. In this particular case ($\gamma = 0$), the bifurcation occurring at $a = 1$ is a *degenerate* fold border collision bifurcation because at the bifurcation there is a whole segment of fixed points (all the points of the segment [0, 1]), but it is followed by only two fixed points—the unstable x_L^* and the second fixed point x_R^* which may be stable or unstable depending on the value of b, as noted above. The bifurcation diagrams in the (a, b) parameter plane in the generic case $\gamma > 0$ are similar, and for $\gamma > 0$ the BCB occurring at $a = 1$ is not degenerate (as can be seen from Fig. 1b, the two fixed points appear close to each other).

Apart from the BCB occurring at $a = 1$, we shall see that the possible dynamic outcomes are finite in number and we can classify and describe all the occurrences. Either one (unique) attracting k-cycle q_k exists (for any integer $k \geq 1$, $q_1 = x_R^*$), or robust chaos in suitable intervals occurs. The chaotic intervals can be properly classified in $2k$-cyclical chaotic intervals Q_{2k} or k-cyclical chaotic intervals Q_k for any $k \geq 1$. An example of a two-dimensional bifurcation diagram is shown in Fig. 2, where only portions of periodicity regions associated with the k-cycle for $k = 1, 2, 3, 4$ are visible, but similar regions exist for any integer k, visible at higher values of b.

Notice that while the BCB occurring at $a = 1$ can be completely characterized using the results of the piecewise linear map, the bifurcations occurring for $a > 1$ are the object of the present paper, and the analysis here performed with a hyperbola as decreasing function, may be repeated with any other decreasing function $g(x)$. Clearly, with a different decreasing function we do not expect to have degenerate flip bifurcations, as those described in Subsection 2.1, but a destabilization via standard flip bifurcations will have no influence on the steps described in Section 4.

Let us first determine some basic properties of the map under study. For the linear function on the left side, from $f(x_L^*) = x_L^*$, we have a fixed point $0 \leq x_L^* < 1$ given by:

$$x_L^* = \frac{\gamma}{a + \gamma - 1} \tag{4}$$

while on the right side of the kink point, from $g(x_R^*) = x_R^*$ a fixed point $x_R^* > 1$ is given by:

$$x_R^* = 1 + \frac{a-1}{b} \tag{5}$$

As already noted, from the slope of the linear function we have that when the fixed points exist, x_L^* is always unstable (as $a > 1$ and $f'(x_L^*) = (a + \gamma) > 1$). Thus initial conditions $x < x_L^*$ have divergent trajectories (to $-\infty$), and bounded dynamics exist only as long as initial conditions $x > x_L^*$ have trajectories which persist to be on the right side of this unstable fixed point x_L^*. So an invariant absorbing interval exists, given by

$$I = [g^2(1), g(1)] = \left[\frac{a^2}{1 + b(a-1)}, a\right] \tag{6}$$

as long as $g^2(1) > x_L^*$, that is for:

$$a^2 > \gamma(-(a+1) + b).$$

This condition is certainly satisfied for $b \leq (a+1)$, while in the case $b > (a+1)$, which, as we shall see below, is the range that interests us, the condition becomes

$$\gamma < \frac{a^2}{b - (a+1)} \tag{7}$$

When $g^2(1) > x_L^*$ then the trajectory of any initial condition $x > x_L^*$ enters the absorbing interval I in a finite number of iterations, while when the condition $g^2(1) < x_L^*$ holds, then we have almost all divergent dynamics. From the shape on the map, which is unimodal in the absorbing interval I, we can see that the homoclinic bifurcation occurring when $g^2(1) = x_L^*$ leads to the destruction of the absorbing interval. This bifurcation can be compared to that occurring in the standard logistic map $f(x) = \mu x(1 - x)$ at $\mu = 4$, for $\mu > 4$ almost all the trajectories are divergent, leaving an invariant Cantor set of points on which the restriction of the map is chaotic.

The basin of attraction of the absorbing interval I includes the non diverging points on the right side of x_L^*. Thus, if there is no other rank-1 preimage of the fixed point x_L^*, which is indeed the case if $x_L^* < (a/b)$, then the basin of attraction is $\mathcal{B}(I) =]x_L^*, +\infty[$, otherwise we have $\mathcal{B}(I) =]x_L^*, g^{-1}(x_L^*)[$.

Considering that

$$x_L^* < \frac{a}{b} \quad \text{if } \gamma < \frac{a(a-1)}{b-a} \tag{8}$$

and $g^{-1}(x_L^*) = \gamma(1-b)/((a-1) + \gamma(1-b))$ we can conclude that for $\gamma < [a(a-1)/(b-a)]$ (resp. >) the basin is given by $\mathcal{B}(I) =]x_L^*, +\infty[$ (resp. $\mathcal{B}(I) =]x_L^*, \gamma(1-b)/((a-1) + \gamma(1-b))[$). We have so proved the following

Proposition 1. *$I = [g^2(1), g(1)] = [(a^2/(1 + b(a-1)), a]$ is an invariant absorbing interval for the map given in (1) and (2)with basin of attraction $\mathcal{B}(I) =]x_L^*, +\infty[$ for $0 \leq \gamma < [a(a-1)/(b-a)]$ and $(I) =]x_L^*, g^{-1}(x_L^*)[=]x_L^*, (\gamma(1-b))/((a-1) + \gamma(1-b))[$ for $a(a-1)/(b-a) \leq \gamma < a^2/(b-(a+1))$. For $\gamma > a^2/(b-(a+1))$ almost all the trajectories are divergent.*

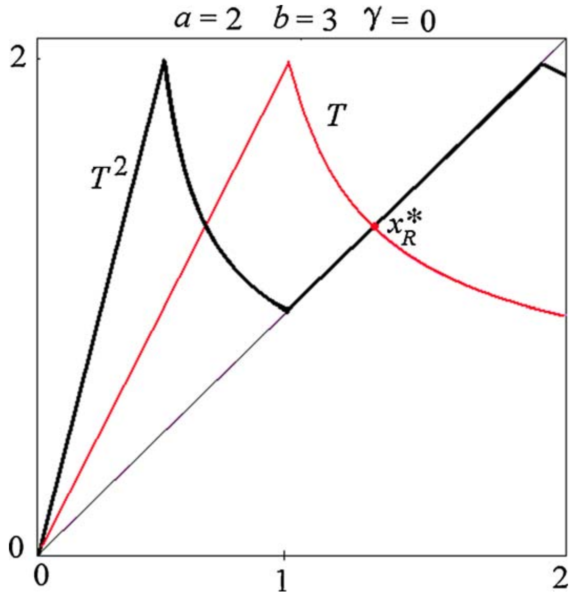

Fig. 3. T and T^2.

2.1. Degenerate flip bifurcations

Regarding the other fixed point, from (3) we have

$$g'(x_R^*) = -\frac{b-1}{a} < 0 \tag{9}$$

so that the fixed point on the right side may be stable or unstable, depending on the parameters (a, b). The fixed point is attracting for $g'(x_R^*) > -1$ i.e. if

$$b < (1+a) \tag{10}$$

in which case the fixed point x_R^* is the only invariant attracting set, it is globally attracting in I and its basin of attraction is the basin $\mathcal{B}(I)$ detected above.

A *degenerate flip bifurcation* occurs at $b=(1+a)$ when we have $g'(x_R^*) = -1$ and $g^2(1)=1$, which means (as we shall prove here below) that at the bifurcation value all the points of the interval I are cycles of period 2 (except for the fixed point), as shown in Fig. 3. After the bifurcation only one attracting 2-cycle is left, which is attracting for the parameters in a suitable region. This stable 2-cycle in turn will undergo a degenerate flip bifurcation which, however, will lead to an unstable 4-cycle belonging to the attracting set, which consists in 4-cyclical chaotic intervals. This is the main property that distinguishes the dynamics of the present linear-hyperbolic model from those of the one-dimensional piecewise linear map. In fact, while for the piecewise linear map the 2-cycle can bifurcate to attracting 2^n cyclical chaotic intervals for any $n>0$, this property is lost in the case of a linear-fractional model.

Let us first show this property of degeneracy occurring at the bifurcation value of the fixed point x_R^*. Considering the second iterate of the function $g(x)$:

$$g^2(x) = \frac{a^2 x}{b(1-b+a)x + (b-1)^2}$$

we can see that when $b=(1+a)$ we have $g^2(x)=x$ for all the points of the interval $I=[g^2(1), g(1)]=[1, a]$ which leads to the conclusion stated above.

After the degenerate flip bifurcation of the fixed point, for $b>(1+a)$ the infinitely many 2-cycles disappear except for one 2-cycle, which is left, with one periodic point on the right and one on the left of the kink point $x=1$ (the distance between the two points of the left 2-cycle is equal to the length of the invariant interval at the bifurcation value). This unique 2-cycle may be attracting for b not too far from $(1+a)$, in which case we shall also find a degenerate flip bifurcation of this 2-cycle. In order to determine the periodic points $\{x_L, x_R\}$ of the 2-cycle we have to solve the system

$$\begin{cases} f(x_L) = x_R \\ g(x_R) = x_L \end{cases} \tag{11}$$

that is:

$$\begin{cases} (a+\gamma)x_L - \gamma = x_R \\ \dfrac{ax_R}{1+b(x_R-1)} = x_L \end{cases} \tag{12}$$

$$\begin{cases} (a+\gamma)x_L - \gamma = x_R \\ x_L^2 b(a+\gamma) + x_L(1-b(\gamma+1)-a(a+\gamma)) + a\gamma = 0 \end{cases} \tag{13}$$

Let us first consider the simplest case with $\gamma = 0$, for which the explicit solution for x_L is immediate and we have that the periodic points $\{x_L, x_R\}$ of the 2-cycle are as follows:

$$x_L = \frac{a^2+b-1}{ab}, \quad x_R = \frac{a^2+b-1}{b} \tag{14}$$

Moreover, in this simplified case we can explicitly determine the eigenvalue of the 2-cycle, which is given by $\lambda_2 = f'(x_L)g'(x_R)$, that is (considering that $b(x_R-1) = (a^2-1)$):

$$\lambda_2 = \frac{-a^2(b-1)}{[1+b(x_R-1)]^2} = -\frac{(b-1)}{a^2} < 0 \tag{15}$$

Thus, in this simplified case ($\gamma = 0$) the 2-cycle is stable as long as $\lambda_2 = -((b-1)/a^2) > -1$, i.e.

$$b < 1 + a^2 \tag{16}$$

Let us prove that at $b = 1 + a^2$ a degenerate flip bifurcation of the 2-cycle occurs. Considering the iterates of the kink point $x = 1$, the 4 points $T^k(1)$, for $k = 1, 2, 3, 4$ are given by

$$\begin{aligned} T^1(1) &= a = f(1) = g(1) \\ T^2(1) &= g(a) = g^2(1) = \frac{a^2}{1+b(a-1)} < 1 \\ T^3(1) &= f(g^2(1)) = \frac{a^3}{1+b(a-1)} \\ T^4(1) &= g(f(g^2(1))) = \frac{a^4}{1+b(a-1)+b(a-1)(a^2+a+1-b)} \end{aligned} \tag{17}$$

and these four points determine the boundaries of two intervals on which we have all cycles of period 4, except for the fixed point and the 2-cycle given above (see Fig. 4). In fact, let us consider a generic point of the interval $J = [T^2(1), T^4(1)] = [g^2(1), g(f(g^2(1)))]$. Then we show that at $b = 1 + a^2$ we have $T^4(x) = (g \circ f)^2(x) = x$, for any $x \in J$. From $g \circ f(x) = [a^2x/(1 + b(ax - 1))]$ we have

$$(g \circ f)^2(x) = \frac{a^4x}{1+b(ax-1)} \cdot \frac{1}{1+b(a^3x/(1+b(ax-1)))} = \frac{a^4x}{[1-b+bax](1-b)+ba^3x} \tag{18}$$

now let us assume $b = 1 + a^2$ so that

$$\begin{aligned} (g \circ f)^2(x) &= \frac{a^4x}{[-a^2+(a+a^3)x](-a^2)+(a^3+a^5)x} = \frac{a^4x}{a^3[a-(1+a^2)x]+a^3(1+a^2)x} \\ &= \frac{ax}{a-(1+a^2)x+(1+a^2)x} = x \end{aligned} \tag{19}$$

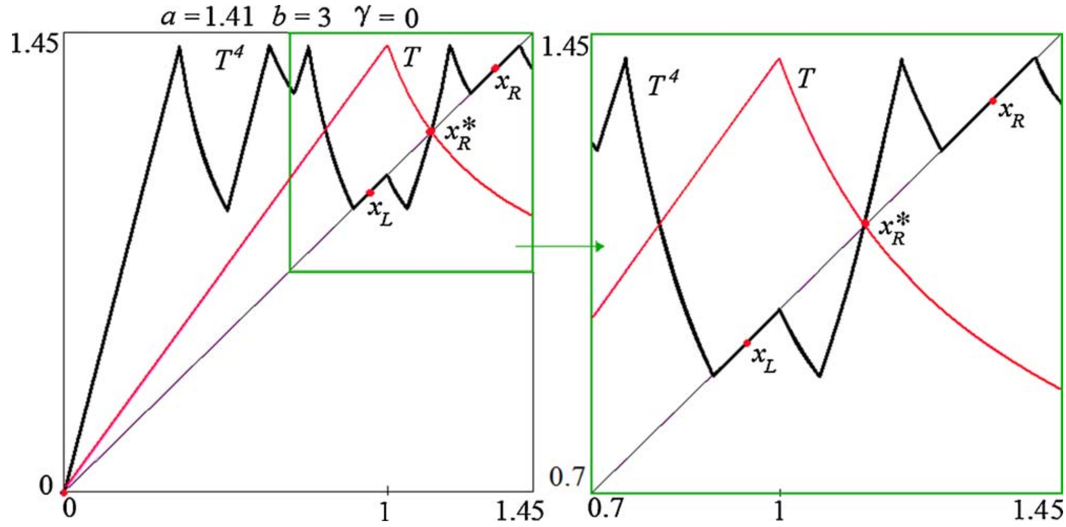

Fig. 4. Degenerate flip bifurcation of the 2-cycle.

Regarding the dynamics that may occur after the degenerate bifurcation at $b = 1 + a^2$, a 4-cycle is certainly created, with one periodic point lower than 1 and three periodic points higher than 1. If we consider the eigenvalue of the 4-cycle at the bifurcation $b = 1 + a^2$, with periodic points $\{1, a, g(a), f(g(a)) = a^3/(1 + b(a - 1))\}$ whose eigenvalue is given by

$$\lambda_4 = f'(g(a))g'(1)g'(a)g'\left(\frac{a^2}{1 - a + a^2}\right) = ag'(1)g'(a)g'\left(\frac{a^3}{1 + b(a - 1)}\right) = -a^2 < -1 \tag{20}$$

we can see that the 4-cycle is unstable whenever it exists. Thus, after the degenerate bifurcation of the 2-cycle we can never obtain a stable 4-cycle. Instead, the dynamics will be chaotic in 4-cyclical intervals.

Let us now turn to the general case $\gamma > 0$. We shall have similar results, although the analytical expressions become more complicated. For example, from the equation in (13) we have that the periodic points of the 2-cycle are given by

$$x_L = \frac{(b(\gamma + 1) + a(a + \gamma) - 1) + \sqrt{D}}{2b(a + \gamma)}$$
$$x_R = (a + \gamma)x_L - \gamma \tag{21}$$

where

$$D = (b(\gamma + 1) + a(a + \gamma) - 1)^2 - 4ab\gamma(a + \gamma)$$

Notice, however, that the flip bifurcation of the fixed point x_R^* is independent of the value of the parameter γ, so that the first degenerate flip bifurcation always occurs at $b = 1 + a$, and at this bifurcation the interval $I = [1, a]$ (whose points belong to cycles of period 2), has a contact with the kink point $x = 1$. As the parameter b is decreased, the same bifurcation can be considered as a border collision bifurcation of the 2-cycle, having one point smaller than 1 and one point higher than 1. From this perspective we can have the eigenvalue of the 2-cycle at the border collision bifurcation, given by $\lambda_2 = f'(x_L)g'(a)$. Considering the bifurcation (at $b = 1 + a$) we get:

$$\lambda_2 = \frac{-(a + \gamma)a(b - 1)}{[1 + b(a - 1)]^2} = -\frac{(a + \gamma)}{a^2} \tag{22}$$

so that for $\gamma = 0$ the eigenvalue is $\lambda_2 = -1/a > -1$ while for $\gamma > 0$ the eigenvalue of the 2-cycle may be smaller than -1, and this is indeed the case for $\gamma > a^2 - a$, that is, for

$$1 < a < a^*, a^* = \frac{1 + \sqrt{1 + 4\gamma}}{2} \tag{23}$$

which means that the degenerate flip bifurcation of the fixed point leads directly to an unstable 2-cycle. In this case, noticing that bounded dynamics exist (as the condition given in Proposition 1 is satisfied), the attracting set is chaotic in some invariant intervals, which may be 4-cyclical, or 2-cyclical or in a unique piece. We have thus proved the following

Proposition 2. *For the map given in (1) and (2)at $b = 1 + a$ a degenerate flip bifurcation of the fixed point $x_R^* = 1 + (a-1)/b$ occurs.*

For $\gamma = 0$ it leads to the stable 2-cycle $\{x_L, x_R\} = \{(a^2+b-1)/ab, (a^2+b-1)/b\}$ and at $b = 1 + a^2$ a degenerate flip bifurcation of the 2-cycle $\{x_L, x_R\}$ occurs, followed by 4-cyclical chaotic intervals.

For $\gamma > 0$ and $a > a^* = (1+\sqrt{1+4\gamma})/2$ it leads to the stable 2-cycle $\{x_L, x_R\}$ given in (21).

For $\gamma > 0$ and $1 < a < a^* = (1+\sqrt{1+4\gamma})/2$ it leads directly to chaotic intervals (4-cyclical or 2-cyclical or in one piece, depending on the value of a).

So what can we say in general about the dynamics occurring after the degenerate flip bifurcation of the 2-cycle? While for the piecewise linear map the bifurcation of the 2-cycle can lead to attracting 2^n-cyclical chaotic intervals for any $n > 0$, here the 2-cycle has the same fate as any other k-cycle that can appear stable, for $k \geq 3$. That is, we can have only $2k$-cyclical chaotic intervals Q_{2k} or k-cyclical chaotic intervals Q_k for any $k \geq 1$.

In order to simplify the exposition in the next section we shall completely analyze the case associated with $\gamma = 0$.

3. Particular case $\gamma = 0$

From the two-dimensional bifurcation diagram in Fig. 2 we can see that outside the stability region of the 2-cycle, there is a transition to cyclical chaotic intervals. That is, for $b > 1 + a^2$ inside the interval I only one cycle of period 4 is left, which is unstable. Moreover, we can see that $(T^4)'(x) > 1$ in all the points of the absorbing interval I, which implies that *no stable cycle can exist for the map T^4 and thus for T*. It follows that all the dynamics are chaotic in cyclical chaotic intervals, which can be 4-cyclical chaotic intervals Q_4, 2-cyclical chaotic intervals Q_2 or one piece chaotic interval Q_1 of *strict chaos* or *full measure chaos* (following [11]) and *robust chaos* (following [4]), i.e. persistent as the parameters are changed. The homoclinic bifurcation leading from Q_4 to Q_2 occurs when the iterates of the kink point merge in the unstable 2-cycle, that is for $T^5(1) = g^2 \circ f \circ g^2(1) = x_R$ (where $x_R = (a^2+b-1)/b$), and we get the following condition:

$$ba^5 - (a^2+b-1)[(1-b)^3 + ba^4 + b(1-b)a^3 + b(1-b)^2 a] = 0 \tag{24}$$

The homoclinic bifurcation leading from 2-cyclical chaotic intervals Q_2 to one chaotic interval Q_1 occurs when the images of the kink point merge in the unstable fixed point x_R^*, that is when $T^3(1) = x_R^*$, i.e. $f \circ g^2(1) = (1 + (a-1)/b)$, which gives:

$$b = \frac{1}{2}(a^2 + 2 + a\sqrt{a^2+4}) \tag{25}$$

Moreover, as occurs in piecewise linear maps, in suitable regions of the parameter plane (a, b) we may have other periodicity regions associated with (stable) maximal k-cycles, having one point in the right side $(x > 1)$ and $k - 1$ points in the left side $(x < 1)$, for any $k \geq 3$. The case with two cycles of period 3 is shown in Fig. 5, as fixed points of the map $T^3(x)$. Differently from the 2-cycle, which appears at the degenerate flip bifurcation (which also is a BCB), we can have *fold border collision bifurcations* leading to the appearance of *a pair* of k-cycles, for any $k \geq 3$. Differently for the fold bifurcations in maps of class $\mathcal{C}^{(1)}$, which from the bifurcation with eigenvalue $\lambda = 1$ necessarily leads to a pair of cycles which are one stable (eigenvalue $0 < \lambda < 1$) and one unstable (eigenvalue $\lambda > 1$), the fold bifurcation in maps not of class $\mathcal{C}^{(1)}$), as in our case, may lead to a similar pair, which we call *saddle-node*, or to a pair on unstable cycles, which we call *saddle-saddle*.

Noticing that our map is unimodal and the critical maximum point is in the kink point $x = 1$, we have that the iterate of the map $T^k(x)$ has a local minimum in the kink point, for any $k > 1$, and that the occurrence of a fold bifurcation, for any $k \geq 3$, always involves also the kink point. That is, at a fold bifurcation two periodic points of the cycles are merging in the kink point (so that it must be a fixed point for the k-th iterate of map: $T^k(1) = 1$). After, when two cycles exist, the two points are separated: on the left of $x = 1$ for one cycle, which we denote by q_k, and on the right of $x = 1$ for the other one, which we denote by q'_k. Being $T(1) > 1$ and $T^2(1) < 1$ we have that the least value of k is $k = 3$, and the cycle denoted q_k must have the periodic points obtained by the following sequence of applications of the functions: $f, g, f, \ldots, f$; and thus it is necessarily a so-called maximal (or principal) cycle. The cycle denoted q'_k must have the periodic points obtained by the following sequence: $g, g, f, \ldots, f$. The cycle which may appear as stable at the fold

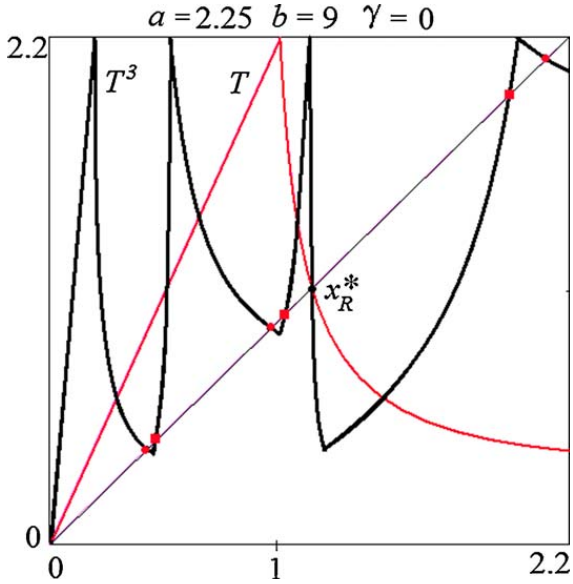

Fig. 5. Graph of the map $T(x)$ and of $T^3(x)$, showing the fixed points and two cycles of period 3.

BCB is the maximal cycle. That is, the fold BCB of type saddle-node gives rise to the unstable cycle q'_k and the stable cycle q_k, while the fold BCB of type saddle-saddle gives rise to the cycles q_k and q'_k—both unstable.

So, in order to detect the equations of the fold BCB for a pair of k-cycles we have to consider the following condition:

$$T^k(1) = f^{k-2} \circ g^2(1) = 1 \tag{26}$$

and we obtain:

$$\frac{a^k}{1 + b(a-1)} = 1 \tag{27}$$

that is:

$$b = \frac{a^k - 1}{a - 1} = (a^{k-1} + \ldots + a + 1) : \Phi_k(a) \tag{28}$$

The fold BCB curves here defined for any $k \geq 3$ also works for $k = 2$, which gives $b = (a + 1)$ corresponding to the BCB of the 2-cycle (and, at the same time, it corresponds in this case to the DFB of the fixed point x_R^*). For $k = 3$ we get $b = (a^2 + a + 1)$ which is the fold BCB of the 3-cycle, and so on. To summarize, for any $k \geq 3$, for $b > \Phi_k(a)$ a pair of cycles exists, q_k and q'_k; q_k may be stable (at least close to the bifurcation) and q'_k is unstable.

Crossing the fold BCB $b = \Phi_k(a)$ when it is saddle-node, as the parameters are varied in the region $b > \Phi_k(a)$ the bifurcation route is as follows:

(i) the stable k-cycle q_k becomes unstable via DFB, leading to $2k$-cyclical chaotic intervals Q_{2k};
(ii) the $2k$-cyclical chaotic intervals Q_{2k} become k-cyclical chaotic intervals Q_k at the first homoclinic bifurcation of q_k, occurring when an iterate of the kink point $x = 1$, $T^{2k}(1)$, merges with the periodic point (i.e. the kink point $x = 1$ is preperiodic to the cycle q_k), also known as internal crisis;
(iii) the k-cyclical chaotic intervals Q_k turn into one piece chaotic interval Q_1 at the first homoclinic bifurcation of q'_k, occurring when an iterate of the kink point $x = 1$, $T^k(1)$, merges with q'_k (i.e. the kink point $x = 1$ is preperiodic to the cycle q'_k), also known as external crisis.

Crossing the fold BCB when it is saddle-saddle, as the parameters are varied in the region $b > \Phi_k(a)$ the BCB leads to the appearance of attracting chaotic intervals bounded by the images of the kink point, which may be $2k$-cyclical or k-cyclical or a unique chaotic interval $Q_1 = [T^2(1), T(1)]$.

On the BCB curve $b = \Phi_k(a)$, the point separating the saddle-node branch from the saddle-saddle one is the intersection point with the flip bifurcation curve of the k-cycle q_k (and will be determined below).

Fig. 2b provides an example in the BCB of the 3-cycle: crossing the curve $b=\Phi_3(a)$ entering the colored region, the bifurcation is a saddle-node, while crossing it entering the white region we have chaotic intervals. The three arrows illustrate the transition to 6-cyclical Q_6, 3-cyclical Q_3 and a unique chaotic interval $Q_1=[T^2(1), T(1)]$.

The flip bifurcation curves and the homoclinic bifurcation curves can be obtained analytically once we have the analytical expression of the periodic points of the cycles (otherwise the steps described above can be detected numerically). As described above, to determine the analytical expression of the periodic point of the k-cycle q_k immediately to the left of the kink point, say x_{1,q_k}, we have to solve the following implicit equation:

$$f^{k-2}\circ g\circ f(x_{1,q_k}) = x_{1,q_k} \tag{29}$$

After some algebra we get

$$x_{1,q_k} = \frac{a^k+b-1}{ab} \tag{30}$$

and the eigenvalue of the cycle q_k is given by

$$\lambda(q_k) = \frac{-(b-1)}{a^k} < 0 \tag{31}$$

so that the flip bifurcation occurs when $\lambda(q_k)=-1$ at:

$$b = 1 + a^k \tag{32}$$

and it is degenerate due to the fact that the component functions $f(x)$ and $g(x)$ are only linear and hyperbolic and their composition for any order is of the same kind. Thus ultimately the flip bifurcation of a fixed point of the map $T^k(x)$ refers to an hyperbolic function, for which the flip bifurcation is degenerate (see [35]).

We can also see that the intersection point between the BCB curve $b=\Phi_k(a)$ and the DFB of q_k occurs when both (28) and (32) are satisfied: $1+a^k=(a^k-1)/(a-1)$, that is for:

$$a^{k-1} = \frac{a^{k-1}-1}{a-1}. \tag{33}$$

Let a_F be the value of a satisfying the equation in (33), then for $a>a_F$ the fold BCB is saddle-node while for $1<a<a_F$ the fold BCB is saddle-saddle. For example, for $k=3$ we get the point

$$a_F = \frac{1+\sqrt{5}}{2}, \quad b = 1+\left(\frac{1+\sqrt{5}}{2}\right)^3. \tag{34}$$

The point corresponding to a_F can be seen in Fig. 2 on the BCB curves at the end of the colored regions (separation point between the saddle-node and saddle-saddle BCB).

The periodic point of the k-cycle q'_k immediately on the right side of the kink point, say x_{1,q'_k}, can be determined by solving the following implicit equation:

$$f^{k-2}\circ g^2(x_{1,q'_k}) = x_{1,q'_k} \tag{35}$$

which gives:

$$x_{1,q'_k} = \frac{a^k-(b-1)^2}{b(1+a-b)} \tag{36}$$

and the periodic points of the cycles q_k and q'_k can be used to detect the homoclinic bifurcations causing the qualitative changes in the cyclical chaotic attractors. It is well known that the extrema of the chaotic intervals are given by the images of the kink point $x=1$. Thus the boundaries of the chaotic intervals Q_{2k} are the points $T^i(1)$ for $i=1, \ldots, 2k$, while the boundaries of the chaotic intervals Q_k are the points $T^i(1)$ for $i=1, \ldots, k$. Then the homoclinic bifurcation leading from the cyclical chaotic intervals Q_{2k} to the chaotic intervals Q_k occurs when the point $T^{2k+1}(1)$ merges in the periodic point of the cycle q_k on the right side of the kink point - that is, in the point $ax_{1,q_k}=(a^k+b-1)/b$. Thus for $T^{2k+1}(1)=ax_{1,q_k}$. While the homoclinic bifurcation leading from the cyclical chaotic intervals Q_k to the chaotic

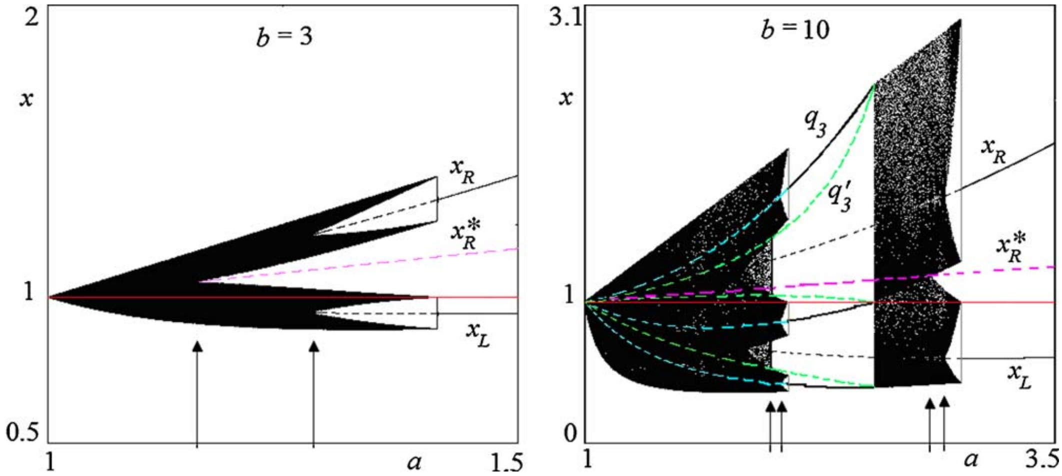

Fig. 6. One dimensional bifurcation diagrams, as a function of the parameter a, at $b = 3$ in (a) and $b = 10$ in (b).

interval Q_1 occurs when the point $T^{k+1}(1)$ merges in the rightmost periodic point of the cycle q_k'- that is, in the point $g(x_{1,q_k'}) = (a^k - (b-1)^2)/(ba^{k-1} - b(b-1))$. To summarize, we have proved the following

Proposition 3. *Consider the map $T(x)$ given in (1), then*

- *the BCB of a pair of k-cycles, $k \geq 3$, occurs at $b = \Phi_k(a) = (a^k - 1)/(a - 1)$; for $a > a_F$ it is saddle-node while for $1 < a < a_F$ it is saddle-saddle, where a_F satisfies (32);*
- *the periodic points of the k-cycles q_k and q_k' immediately on the right side of the kink point are given by $ax_{1,q_k} = (a^k + b - 1)/b$ and $x_{1,q_k'} = (a^k - (b-1)^2)/(b(1 + a - b))$, respectively;*
- *the stable cycle q_k becomes unstable via DFB, leading to 2k-cyclical chaotic intervals Q_{2k}, at $b = 1 + a^k$;*
- *the 2k-cyclical chaotic intervals Q_{2k} become k-cyclical chaotic intervals Q_k at the first homoclinic bifurcation of q_k (internal crisis), occurring when the following condition holds: $T^{2k+1}(1) = g \circ f^{k-2} \circ g \circ f^{k-1} \circ g^2(1) = ax_{1,q_k}[= (a^k + b - 1)/b]$;*
- *the k-cyclical chaotic intervals Q_k turn into one piece chaotic interval Q_1 at the first homoclinic bifurcation of q_k' (external crisis), occurring when the following condition holds: $T^{k+1}(1) = f^{k-1} \circ g^2(1) = g(x_{1,q_k'})[= (a^k - (b-1)^2)/(ba^{k-1} - b(b-1))]$.*

Proposition 4. *The two homoclinic bifurcations given in Proposition 3 for $k \geq 3$ also work for the case $k = 2$ assuming $ax_{1,q_k} = x_R = (a^2 + b - 1)/b$ and $g(x_{1,q_k'}) = x_R^*$ (the fixed point).*

From Fig. 2 we can see that at the BCB occurring for $a = 1$ the system can enter immediately into a chaotic regime. In fact, depending on the value of the parameter b, the dynamics may be immediately chaotic in 4-cyclical intervals, or 2-cyclical intervals or in one unique interval. Two one-dimensional bifurcation diagrams are shown in Fig. 6 at $b = 3$ and $b = 10$ fixed and increasing a. For each value of $b > 2$ fixed, as a function of a, only a finite number of the infinitely many existing periodicity regions is crossed. In Fig. 6, as a crosses through the value 1 we have immediately chaotic dynamics inside the invariant absorbing interval Q_1 (and the same occurs for any fixed $b > 3$). Increasing the value of a we observe the sequences explained above in reverse order up to the attracting fixed point. As a is decreased, Fig. 6a illustrates the transition involving only the 2-cycle $\{x_L, x_R\}$. The chaotic intervals Q_4 appear at the DFB of the 2-cycle, and are merging into the chaotic intervals Q_2 at the first homoclinic bifurcation of the 2-cycle, when $T^5(1) = x_R$, while the transition to the chaotic interval Q_1 occurs at the homoclinic bifurcation of the fixed point, when $T^3(1) = x_R^*$.

In the example shown in Fig. 6b, besides the route associated with the 2-cycle, only the route of the 3-cycle occurs. Considering the bifurcation sequence as the parameter a is decreased, at $a = b - 1 = 9$ the fixed point becomes unstable and a stable 2-cycle appears, and as we can see in Fig. 6b, at $a = \sqrt{b-1} = 3$, 4-cyclical chaotic intervals appear, which become 2-cyclic chaotic intervals at the merging with the unstable 2-cycle (black dashed line) and one unique chaotic interval at the merging with the unstable fixed point x_R^*. As the parameter decreases further, a stable 3-cycle q_3

appears by saddle-node border collision bifurcation, and after its degenerate flip bifurcation 6 chaotic intervals emerge, which reduce to three at the merging with the unstable 3-cycle q_3 which flip-bifurcated (dashed line in blue in Fig. 6), and the merging with the unstable 3-cycle q_3' (dashed line in green in Fig. 6) leads to a unique chaotic interval. (For interpretation of the references to color in text, the reader is referred to the web version of the article.)

4. The generic model

In the generic model, for $\gamma > 0$, we have seen that the degenerate flip bifurcation of the two cycle may lead to a stable 2-cycle or directly to chaotic intervals, depending on the value of γ. The slope of the linear function $f(x)$ for $\gamma > 0$ is higher, with respect to the case with $\gamma = 0$, which leads to a quicker transition to chaotic dynamics. After the flip bifurcation of the 2-cycle, we have seen that a 4-cycle can never be stable, and only chaotic dynamics can exist as the derivative $(T^4)'(x)$ for $\gamma > 0$ is necessarily greater or equal to the one occurring for $\gamma = 0$, for which we have $(T^4)'(x) > 1$ in all the points of the absorbing interval I. Thus, also in the generic case we can conclude that no stable cycle of T^4 can exist, and the bounded dynamics cover cyclical chaotic intervals, which, issuing from the 2-cycle, can only be 4-cyclical chaotic intervals Q_4, or 2-cyclical chaotic intervals Q_2 or one piece chaotic interval Q_1 of *robust chaos*.

The homoclinic bifurcation leading from Q_4 to Q_2 occurs, as usual, when the images of the kink point merge in the unstable 2-cycle, that is for $T^5(1) = g^2 \circ f \circ g^2(1) = x_R (= (a^2 + b - 1)/b)$.

The homoclinic bifurcation leading from 2-cyclical chaotic intervals Q_2 to a unique chaotic interval Q_1 occurs when $T^3(1) = f \circ g^2(1) = x_R^*(x_R^* = 1 + (a-1)/b)$.

Clearly, besides the "route" associated with the 2-cycle, for any fixed value $\gamma > 0$, in suitable regions of the parameter plane (a, b) we can have other periodicity regions associated with (stable) maximal k-cycles as we have seen in the case $\gamma = 0$, having one point in the right side $(x > 1)$ and $k - 1$ points in the left side $(x < 1)$, for any $k \geq 3$. In fact, we can perform the same reasoning as in the previous section. Noticing that the map is unimodal with the maximum in the kink point, the map $T^k(x)$ has a local minimum in the kink point, which is involved at a fold bifurcation. At any fold BCB two periodic points of the cycles merge in the kink point, $T^k(1) = 1$, and from $T(1) > 1$ and $T^2(1) < 1$ we have $k \geq 3$. Two cycles exist after the bifurcation: q_k whose periodic points are obtained by applications of the functions: $f, g, f, \ldots, f$; which is a maximal cycle (and may be stable), and the unstable cycle q_k' whose periodic points are obtained by the following sequence: $g, g, f, \ldots, f$. Thus we can have *fold border collision bifurcations (saddle-node or saddle-saddle)* leading to the appearance of *a pair* of k-cycles, for any $k \geq 3$.

The equations of the fold BCB for a pair of k-cycles for any $k \geq 3$ can be obtained by the following condition:

$$T^k(1) = f^{k-2} \circ g^2(1) = 1 \tag{37}$$

In the generic case with $\gamma > 0$ we still have $g^2(1) = g(a) = a^2/(1 + b(a-1))$ and then, using

$$f^n(x) = (a+\gamma)^n x - \gamma \frac{(a+\gamma)^n - 1}{a + \gamma - 1} \tag{38}$$

we have

$$f^{k-2} \circ g^2(1) = f^{k-2}\left(\frac{a^2}{1 + b(a-1)}\right) = (a+\gamma)^{k-2} \frac{a^2}{1 + b(a-1)} - \gamma \frac{(a+\gamma)^{k-2} - 1}{a + \gamma - 1}$$

and the equation of the BCB curves are:

$$(a+\gamma)^{k-2} \frac{a^2}{1 + b(a-1)} - \gamma \frac{(a+\gamma)^{k-2} - 1}{a + \gamma - 1} = 1$$

that is:

$$b = \frac{(a+\gamma)^{k-2} a^2 (a + \gamma - 1) - \gamma (a+\gamma)^{k-2} - (a-1)}{(a-1)[\gamma (a+\gamma)^{k-2} + (a-1)]} =: \Phi_k(a, \gamma) \tag{39}$$

(and clearly for $\gamma = 0$ we get the same expression as above in (28)). Note that the formula in (28) also works for the particular case $k = 2$, that is, for the 2-cycle. In fact we have $\Phi_2(a, \gamma) = 1 + a$, and thus the 2-cycle bifurcates at $b = 1 + a$ as already seen in Section 2.

While for $k \geq 3$ the k-cycles which appear/disappear by BCB when the parameters cross the curves $b = \Phi_k(a, \gamma)$ detected above are in pair, that is, for $b > \Phi_k(a, \gamma)$ a pair of cycles exists, q_k may be stable and q'_k which is always unstable. To determine one periodic point of the k-cycle q_k, let us call, as in the previous section, x_{1,q_k} the periodic point immediately on the left of the kink point, so that we have to solve the following implicit equation:

$$f^{k-2} \circ g \circ f(x_{1,q_k}) = x_{1,q_k} \tag{40}$$

From

$$g(f(x)) = \frac{a((a+\gamma)x-\gamma)}{1+b((a+\gamma)x-\gamma-1)}$$

and considering (38) we have:

$$f^{k-2} \circ g \circ f(x_{1,q_k}) = (a+\gamma)^{k-2}\frac{a((a+\gamma)x_{1,q_k}-\gamma)}{1+b((a+\gamma)x_{1,q_k}-\gamma-1)} - \gamma\frac{(a+\gamma)^{k-2}-1}{a+\gamma-1}$$

so that we have to solve

$$(a+\gamma)^{k-2}\frac{a((a+\gamma)x_{1,q_k}-\gamma)}{1+b((a+\gamma)x_{1,q_k}-\gamma-1)} - \gamma\frac{(a+\gamma)^{k-2}-1}{a+\gamma-1} = x_{1,q_k} \tag{41}$$

While for the k-cycle q'_k let x_{1,q'_k} be the periodic point immediately on the right side of the kink point, then it can be determined solving the following implicit equation:

$$f^{k-2} \circ g^2(x_{1,q'_k}) = x_{1,q'_k} \tag{42}$$

From

$$g^2(x) = \frac{a^2x}{(1-b)^2+bx(1+a-b)}$$

and considering (38) we have:

$$f^{k-2} \circ g \circ f(x_{1,q'_k}) = (a+\gamma)^{k-2}\frac{a^2x_{1,q'_k}}{(1-b)^2+bx_{1,q'_k}(1+a-b)} - \gamma\frac{(a+\gamma)^{k-2}-1}{a+\gamma-1}$$

so that we have to solve

$$(a+\gamma)^{k-2}\frac{a^2x_{1,q'_k}}{(1-b)^2+bx_{1,q'_k}(1+a-b)} - \gamma\frac{(a+\gamma)^{k-2}-1}{a+\gamma-1} = x_{1,q'_k} \tag{43}$$

It is plain that setting $\gamma = 0$ in the equations given in (41) and (43) the solutions that we obtain are the periodic points already given in (30) and (36), respectively.

When the fold BCB is saddle-node, then the stable cycle q_k becomes unstable via degenerate flip bifurcation, leading to $2k$-cyclical chaotic intervals Q_{2k}.

When the fold BCB is saddle-saddle it may lead directly to cyclical chaotic intervals Q_{2k} or to cyclical chaotic intervals Q_k or to Q_1.

The chaotic intervals Q_{2k} merge into the chaotic intervals Q_k at the homoclinic bifurcation of the k-cycle q_k, occurring when $T^{2k+1}(1) = g \circ f^{k-2} \circ g \circ f^{k-1} \circ g^2(1) = ax_{1,q_k}$.

The chaotic intervals Q_k become a unique chaotic interval Q_1 at the homoclinic bifurcation of the k-cycle q'_k, occurring when $T^{k+1}(1) = f^{k-1} \circ g^2(1) = g(x_{1,q'_k})$.

The bifurcation curves described above can be detected numerically.

5. Conclusions

In this paper we have investigated the dynamics which can occur in a continuous one-dimensional linear-hyperbolic model. We have seen the persistence of some properties already known to exist in piecewise linear continuous maps. We have determined the fold BCB of pair of k-cycles q_k and q'_k, and the degenerate flip bifurcations of the stable k-cycles

q_k followed by $2k$-cyclical chaotic intervals Q_{2k}. Then we have determined the homoclinic bifurcations leading to k-cyclical chaotic intervals Q_k and to a unique chaotic interval Q_1 for any $k \geq 3$. A new dynamic behavior concerns the 2-cycle which appears by degenerate flip of the fixed point x_R^* on the right side of the kink point, which also is a BCB of a 2-cycle. We have shown that it is not possible to have regions in the parameter space with attracting 2^n-cyclical chaotic intervals for any $n > 0$. Here the bifurcation of the 2-cycle has the same fate as any other k-cycle which can appear stable, for $k \geq 3$. That is, we can have only $2k$-cyclical chaotic intervals Q_{2k} or k-cyclical chaotic intervals Q_k for any $k \geq 1$. Moreover this sequence of bifurcation depends on the value of the parameter γ. For positive values of γ the degenerate flip bifurcation of x_R^* may be followed directly by chaotic intervals Q_4 or Q_2 or Q_1.

References

[1] V. Avrutin, M. Schanz, On multi-parametric bifurcations in a scalar piecewise-linear map, Nonlinearity 19 (2006) 531–552.
[2] V. Avrutin, M. Schanz, S. Banerjee, Codimension-3 bifurcations: explanation of the complex 1-, 2- and 3d bifurcation structures in nonsmooth maps, Physical Review E 75 (2007) 066205.
[3] V. Avrutin, P.S. Dutta, M. Schanz, S. Banerjee, Influence of a square-root singularity on the behavior of piecewise smooth maps, Nonlinearity 23 (2010) 445–463.
[4] S. Banerjee, J.A. Yorke, C. Grebogi, Robust chaos, Physical Review Letters 80 (1998) 3049–3052.
[5] S. Banerjee, C. Grebogi, Border-collision bifurcations in two-dimensional piecewise smooth maps, Physical Review E 59 (1999) 4052–4061.
[6] S. Banerjee, M.S. Karthik, G.H. Yuan, J.A. Yorke, Bifurcations in one-dimensional piecewise smooth maps—theory and applications in switching circuits, IEEE Transactions on Circuits and Systems: I 47 (2000) 389–394.
[7] S. Banerjee, G.C. Verghese, Nonlinear Phenomena in Power Electronics: Attractors, Bifurcations, Chaos, and Nonlinear Control, IEEE Press, New York, 2001.
[8] H. Dankowicz, A.B. Nordmark, On the origin and bifurcations of stick-slip oscillations, Physica D 136 (2000) 280–302.
[9] R.H. Day, Irregular growth cycles, American Economic Review 72 (1982) 406–414.
[10] R.H. Day, Complex Economic Dynamics, MIT Press, Cambridge, MA, 1994.
[11] R.H. Day, G. Pianigiani, Statistical dynamics and economics, Journal of Economic Behavior and Organization 16 (1991) 37–84.
[12] M. di Bernardo, M.I. Feigin, S.J. Hogan, M.E. Homer, Local analysis of C-bifurcations in ndimensional piecewise smooth dynamical systems, Chaos Solitons & Fractals 10 (1999) 1881–1908.
[13] M. di Bernardo, C.J. Budd, A.R. Champneys, P. Kowalczyk, Piecewise-smooth Dynamical Systems: Theory and Applications, Applied Mathematical Sciences 163, Springer-Verlag, London, 2007.
[14] S. Foale, S.R. Bishop, Bifurcations in impact oscillations, Nonlinear Dynamics 6 (1994) 285–299.
[15] L. Gardini, I. Sushko, A. Naimzada, Growing through chaotic intervals, Journal of Economic Theory 143 (2008) 541–557.
[16] C. Halse, M. Homer, M. di Bernardo, C-bifurcations and period-adding in one-dimensional piecewise-smooth maps, Chaos Solitons & Fractals 18 (2003) 953–976.
[17] J. Ing, E. Pavlovskaia, M. Wiercigroch, S. Banerjee, Experimental study of impact oscillator with one-sided elastic constraint, Philosophical Transactions of the Royal Society of London, Series A 366 (2008) 679–704.
[18] N.N. Leonov, Map of the line onto itself, Radiofisica 3 (1959) 942–956.
[19] N.N. Leonov, Discontinuous map of the straight line, Doklady Akademii Nauk SSSR 143 (1962) 1038–1041.
[20] Y.L. Maistrenko, V.L. Maistrenko, L.O. Chua, Cycles of chaotic intervals in a time-delayed Chua's circuit, International Journal of Bifurcation and Chaos 3 (1993) 1557–1572.
[21] Y.L. Maistrenko, V.L. Maistrenko, S.I. Vikul, L.O. Chua, Bifurcations of attracting cycles from time-delayed Chua's circuit, International Journal of Bifurcation and Chaos 5 (1995) 653–671.
[22] Y.L. Maistrenko, V.L. Maistrenko, S.I. Vikul, On period-adding sequences of attracting cycles in piecewise linear maps, Chaos Solitons & Fractals 9 (1998) 67–75.
[23] C. Mira, Chaotic Dynamics, World Scientific, Singapore, 1987.
[24] A.B. Nordmark, Non-periodic motion caused by grazing incidence in an impact oscillator, Journal of Sound and Vibration 145 (1991) 279–297.
[25] H.E. Nusse, E. Ott, J.A. Yorke, Border-collision bifurcations: an explanation for observed bifurcation phenomena, Physical Review E 49 (1994) 1073–1076.
[26] H.E. Nusse, J.A. Yorke, Border-collision bifurcations including period two to period three for piecewise smooth systems, Physica D 57 (1992) 39–57.
[27] H.E. Nusse, J.A. Yorke, Border-collision bifurcation for piecewise smooth one-dimensional maps, International Journal of Bifurcation and Chaos 5 (1995) 189–207.
[28] T. Puu, I. Sushko, Oligopoly Dynamics, Models and Tools, Springer Verlag, New York, 2002.
[29] T. Puu, I. Sushko, Business Cycle Dynamics, Models and Tools, Springer Verlag, New York, 2006.
[30] R. Sharan, S. Banerjee, Character of the map for switched dynamical systems for observations on the switching manifold, Physics Letters A 372 (2008) 4234–4240.
[31] D.J.W. Simpson, J.D. Meiss, Neimark–Sacker bifurcations in planar, piecewise-smooth, continuous maps, SIAM Journal on Applied Dynamics Systems 7 (2008) 795–824.
[32] I. Sushko, A. Agliari, L. Gardini, Bistability and border-collision bifurcations for a family of unimodal piecewise smooth maps, Discrete and Continuous Dynamical Systems Series B 5 (2005) 881–897.

[33] I. Sushko, A. Agliari, L. Gardini, Bifurcation structure of parameter plane for a family of unimodal piecewise smooth maps: Border-collision bifurcation curves, Chaos Solitons & Fractals 29 (2006) 756–770.
[34] I. Sushko, L. Gardini, Center bifurcation for two-dimensional border-collision normal form, International Journal of Bifurcation and Chaos 18 (2008) 1029–1050.
[35] I. Sushko, L. Gardini, Degenerate bifurcations and border collisions in piecewise smooth 1D and 2D maps, International Journal of Bifurcation and Chaos 20 (2010) 2045–2070.
[36] F. Tramontana, L. Gardini, R. Dieci, F. Westerhoff, The emergence of 'Bull and Bear' dynamics in a nonlinear 3d model of interacting markets, Discrete Dynamics in Nature and Society (2009) 310471.
[37] F. Tramontana, L. Gardini, R. Dieci, F. Westerhoff, Global bifurcations in a three dimensional financial model of "bull and bear" interactions, in: C. Chiarella, G.I. Bischie, L. Gardini (Eds.), Nonlinear Dynamics in Economics, Finance and Social Sciences, Springer Verlag, New York, 2009.
[38] Z.T. Zhusubaliyev, E. Mosekilde, Bifurcations and Chaos in Piecewise-Smooth Dynamical Systems, World Scientific, Singapore, 2003.
[39] Z.T. Zhusubaliyev, E. Mosekilde, S. Maity, S. Mohanan, S. Banerjee, Border collision route to quasiperiodicity: numerical investigation and experimental confirmation, CHAOS 16 (2006) 023122.
[40] Z.T. Zhusubaliyev, E. Soukhoterin, E. Mosekilde, Quasiperiodicity and torus breakdown in a power electronic dc/dc converter, Mathematics and Computers in Simulation 73 (2007) 364–377.